OAK RIDGE NATIONAL LABORATORY LIBRARIES
3 4456 0551009 7

ORNL/TM-5697

cy 2

Production of Homogeneous Titanium–Hastelloy N Alloys

D. N. Braski
J. M. Leitnaker

OAK RIDGE NATIONAL LABORATORY
CENTRAL RESEARCH LIBRARY
DOCUMENT COLLECTION
LIBRARY LOAN COPY
DO NOT TRANSFER TO ANOTHER PERSON
If you wish someone else to see this document, send in name with document and the library will arrange a loan.
UCN-7969
(3 3-67)

OAK RIDGE NATIONAL LABORATORY
OPERATED BY UNION CARBIDE CORPORATION FOR THE ENERGY RESEARCH AND DEVELOPMENT ADMINISTRATION

Printed in the United States of America. Available from
National Technical Information Service
U.S. Department of Commerce
5285 Port Royal Road, Springfield, Virginia 22161
Price: Printed Copy $4.00; Microfiche $3.00

This report was prepared as an account of work sponsored by the United States Government. Neither the United States nor the Energy Research and Development Administration/United States Nuclear Regulatory Commission, nor any of their employees, nor any of their contractors, subcontractors, or their employees, makes any warranty, express or implied, or assumes any legal liability or responsibility for the accuracy, completeness or usefulness of any information, apparatus, product or process disclosed, or represents that its use would not infringe privately owned rights.

ORNL/TM-5697

Contract No. W-7405-eng-26

METALS AND CERAMICS DIVISION

PRODUCTION OF HOMOGENEOUS TITANIUM–HASTELLOY N ALLOYS

D. N. Braski J. M. Leitnaker

Date Published: February 1977

OAK RIDGE NATIONAL LABORATORY
Oak Ridge, Tennessee 37830
operated by
UNION CARBIDE CORPORATION
for the
ENERGY RESEARCH AND DEVELOPMENT ADMINISTRATION

OAK RIDGE NATIONAL LABORATORY LIBRARIES
3 4456 0551009 7

CONTENTS

ABSTRACT 1

INTRODUCTION 1

MATERIALS AND EXPERIMENTAL PROCEDURES 2

- Casting 2
- Fabrication 2
- Metallography 2
- Transmission Electron Microscopy (TEM) 2
- Carbide Extractions 4
- X-Ray Analysis 4

RESULTS 4

- Memory Effects with Carbide Stringers 4
- Adjustment of Carbon Content 7
- Adjustment of Fabrication Parameters 10

PROPERTIES OF HOMOGENEOUS Ti-HASTELLOY 14

DISCUSSION 17

CONCLUSIONS 17

ACKNOWLEDGMENTS 18

APPENDIX A 18

APPENDIX B 19

PRODUCTION OF HOMOGENEOUS TITANIUM–HASTELLOY N ALLOYS

D. N. Braski J. M. Leitnaker

ABSTRACT

The modification of Hastelloy N by titanium can result in inhomogeneously distributed carbide precipitates. The metallurigical principles necessary to produce a homogeneous alloy are stated and demonstrated. It is shown that a homogeneous alloy leads to more uniform postirradiation properties and, by chance, better properties. A "memory" effect in the alloy is identified and shown to be caused by the inhomogeneities.

INTRODUCTION

Hastelloy N is a nickel-base alloy (16 wt % Mo, 7 wt % Cr, 4 wt % Fe, 0.55 wt % Mn, and 0.06 wt % C) that was developed in the 1950s for the molten-salt reactor. Recently, the alloy composition was modified to obtain improved resistance to radiation damage by adding about 2 wt % Ti to a slightly different Hastelloy N base (13% Mo, 7% Cr, 0.05% C).[1] The microstructure of Ti–Hastelloy N consists of a face-centered cubic (γ) matrix containing face-centered-cubic metallic carbide particles (MC).[2] The carbide particles are usually massive and are usually segregated in the form of stringers. Such carbide stringers are common in many structural materials and are often created when groups of segregated carbide particles in the original casting are extended during fabrication.[3,4] The carbide stringers are often deleterious during working treatments[5] and impart a directionality to mechanical properties of the material.[4] In the case of Ti–Hastelloy N, the stringers are believed to contribute large variations in creep properties. It was the purpose of this investigation to develop a procedure for producing Ti–Hastelloy N free of carbide stringers and thereby reduce the variation in mechanical properties of the alloy.

To achieve this goal, basic metallurgical and thermodynamic principles were used in an attempt to dissolve the reportedly stable MC-type carbides[6–8] and retain them in solution during fabrication. This could be done in two different ways. The first called for a reduction in carbon content of the alloy such that the carbides would remain in solution using the standard fabrication schedule. The second was based on finding a suitable solution annealing treatment that could be used in Ti–Hastelloy N having a nominal carbon level (~0.06 wt %). If successful, the second approach offers the additional advantage of possibly being able to precipitate a moderate amount of MC uniformly in the alloy microstructure, using subsequent thermal aging treatments, thereby increasing the strength of the alloy. After producing a homogeneous microstructure in Ti–Hastelloy N, specimens of the alloy were irradiated in the Oak Ridge Research Reactor and subsequently creep tested. Other samples were corrosion tested to determine the resistance of the homogeneous alloy to grain boundary embrittlement by the fission product tellurium.[9]

---

1. H. E. McCoy, Jr., and J. R. Weir, Jr., "Development of Titanium-Modified Hastelloy with Improved Resistance to Radiation Damage," *Irradiation Effects in Structural Alloys for Thermal and Fast Reactors,* ASTM STP-457 (1969), pp. 290–311.
2. D. N. Braski, J. M. Leitnaker, and G. A. Potter, "Microstructural Analysis of Titanium-Modified Hastelloy N," *MSR Program Semiannu. Prog. Rep. Aug. 31, 1975,* ORNL-5078, pp. 84–91.
3. R. A. Grange, "Microstructural Alterations in Iron and Steel During Hot Working," *Proc. 9th Sagamore Army Matls. Res. Conf., Raquette Lake, N.Y., Aug. 28–31, 1962,* Syracuse University Press, 1964.
4. N. E. Woldman, *Metal Process Engineering,* Reinhold, New York, 1948, pp. 82–87.
5. *ASM Metals Handbook,* vol. 5, 1970, p. 114.
6. R. F. Decker and C. T. Sims, "The Metallurgy of Ni-Base Alloys," *The Superalloys,* ed. C. T. Sims and W. G. Hagel, Wiley, New York, 1972, p. 52.
7. W. Betteridge, *The Nimonic Alloys,* Edward Arnold, London, 1959, pp. 29, 68, 88.
8. H. E. Collins, "Relative Long-Time Stability of Carbide and Intermetallic Phases in Nickel-Base Superalloys," *Trans. ASM* **62,** 82–104 (1969).
9. H. E. McCoy, "Intergranular Cracking of Structural Materials Exposed to Fuel Salt," *MSR Program Semiannu. Prog. Rep. Aug. 31, 1972,* ORNL-4832, p. 63.

MATERIALS AND EXPERIMENTAL PROCEDURES

Casting

The alloys were arc melted under argon in a tungsten-electrode arc melter at a pressure of 20 torr. The amount of chromium in the original charge was 0.5% higher than specified for the alloy to allow for evaporation losses. A zirconium charge was melted in the apparatus just prior to melting of the alloy to getter residual gases in the environment. Each alloy was melted six times, with a total melt time of less than 5 min. Finally, the alloy button was remelted and drop cast into a water-cooled, cylindrical copper mold. The nominal compositions of the Ti–Hastelloy N alloys used in the investigation are given in Table 1.

Table 1. Alloy compositions (wt %)

Element	Alloy				
	452	451	450	503	114
Mo	13.5	13.5	13.6	12.95	12.03
Cr	7.7	8.2	8.1	6.96	7.24
Ti	1.8	1.9	2.1	1.94	1.96
C	0.055	0.038	0.062	0.06	0.05
Mn	<0.1	<0.1	<0.1	<0.1	<0.1
Nb	<0.1	<0.1	<0.1	<0.1	<0.1
Fe	~0.3	~0.3	~0.3	~0.3	~0.3
Ni	Balance	Balance	Balance	Balance	Balance

Fabrication

The 6-in.-long × 1-in.-diam ingots were converted into $^1/_4$-in.-diam rods. The schedules used to fabricate the Ti–Hastelloy N alloys 450, 451, and 452 are listed in Table 2. Alloy 451 had a carbon content of 0.038 wt % and was fabricated in our facility by the established process for Hastelloy N alloys. Several slight modifications in annealing times were used for alloy 452 (0.055 wt % C). The schedule for alloy 450 was designed to eliminate stringers and differs from the standard schedule mainly in the use of a higher-temperature homogenizing anneal. To minimize decarburization at the high homogenizing temperatures, the 450 ingot was canned in a type 316 stainless steel tube having a 0.120-in. wall.

Metallography

Samples for metallographic examination were cut on a water-cooled, high-speed, abrasive cutoff wheel and mounted in epoxy (Araldite). A small wire conductor was spot welded to the back of the sample to permit electrolytic etching. The samples were polished in vibratory units, using alumina first and then diamond-polishing compounds. Samples were electrolytically etched for ~20 sec in a solution of 10 g of oxalic acid in 100 ml of H_2O, at room temperature, using a dc potential of ~2 V.

Transmission Electron Microscopy (TEM)

Material for TEM was cut into 0.04-cm-thick sheets using a water-cooled, high-speed abrasive cutoff wheel. Disks 0.3 cm in diameter were then punched from the sheet using a steel punch and die. The disks were dimpled by jet polishing[10] to a thickness of ~0.08 mm in a solution of 66 ml of HNO_3 and 133

10. C. K. H. DuBose and J. O. Stiegler, *Semiautomatic Preparation of Specimens for Transmission Electron Microscopy*, ORNL-4066 (February 1967).

Table 2. Fabrication schedule for 2% Ti–Hastelloy N alloys (450–452)

Step No.	Fabrication process	Diam (in.)	Reduction of area (%)	451 (0.038 wt % C)	452 (0.055 wt % C)	450 (0.062 wt % C)
1	Arc-drop cast	1.00				
2	Hot swage at 1177°C					
	Pass 1	0.87	24.3	15-min reheat between passes	30-min reheat between passes	Canned in 316 SS; 15-min reheat between passes
	Pass 2	0.74	27.7			
	Pass 3	0.64	25.2			
	Pass 4	0.54	28.8			
	Pass 5	0.49	17.7			
	Pass 6	0.43	22.9			
3	Homogenizing anneal			1 hr at 1177°C (air cooled)	2 hr at 1177°C (air cooled)	1 hr at 1260°C (air cooled) + 1 hr at 1300°C (water quenched)
4	Cold swage (room temperature)	0.34	37.5			
5	Intermediate anneal			1 hr at 1177°C	1 hr at 1177°C	15 min at 1177°C
6	Cold swage (room temperature)	0.25	45.9			

ml of methyl alcohol at room temperature. A dc potential of ~200 V and 245 mA was used in jet polishing. The disks were finally electrochemically polished in a solution of 66 ml of HNO_3, 133 ml of methyl alcohol, and 10 ml of H_3PO_4 at −20°C until perforation occurred. Final polishing was at a dc potential of ~50 V.

Carbide Extractions

Carbide particles were extracted from samples by electrochemically dissolving the matrix material in a solution of 10 ml of concentrated HCl and 90 ml of ethyl alcohol at room temperature. A dc potential of 1.5 V was maintained between the sample (anode) and a platinum cathode. The carbides were separated from the solution by centrifuging and then were dried for at least 30 min in a vacuum desiccator. The dried carbides were weighed with a precision of at least 0.06 mg.

X-Ray Analysis

Extracted carbides were analyzed by x-ray diffraction by first combining them with a drop of ethyl alcohol and depositing the slurry on a polished single-crystal substrate of silicon. The silicon crystal was cut so that the surface normal was ~7° off the (111) pole and thus provided a low-background substrate for x-ray diffraction analysis. A graphite monochromator in the diffracted beam further reduced background by eliminating fluorescent radiation. Data were collected on paper tapes via a Teletype readout. The scan speed was $^1/_8°$ 2θ/min. The information on the paper tapes was subsequently recorded on computer cards, and the x-ray profiles were plotted using a Calcomp plotter. The advantage of this plotting procedure is that data can be recorded without operator attention, and small peaks can be examined at a later time after the sample has been discarded. This technique has been shown to provide excellent sensitivity and can be used on as little as ~1 mg of precipitate.

The extracted carbides were also analyzed qualitatively by x-ray fluorescence. The silicon substrate with deposited carbide particles was placed directly in a General Electric diffractometer that had been converted for fluorescence analysis. A silver-target x-ray tube was utilized along with an incident-beam graphite monochromator and silicon solid-state detector.

RESULTS

Memory Effects with Carbide Stringers

A "memory effect" observed with the microstructure of the Ti–Hastelloy N alloys is illustrated by the series of micrographs for alloy 452 shown in Fig. 1. Figure 1(*a*) shows the microstructure of a longitudinal section from an as-swaged 452 rod. The matrix consisted of γ solid solution and carbide stringers. The carbides were extracted and shown by x-ray diffraction to be the fcc, MC type (see Appendix A). X-ray fluorescence showed that "M" consisted mainly of Mo, Ti, and Cr, in order of decreasing amounts. When the 452 sample was solution annealed for 1 hr at 1177°C (a standard annealing treatment for Hastelloy N), most of the carbides were dissolved into the matrix as shown in Fig. 1(*b*). Recrystallization and growth of the cold-worked structure had also taken place as evidenced by the larger, equiaxed grains. The grain boundaries were nonplanar as a result of the pinning action of some residual carbide particles that survived the solution anneal. When the 452 sample was finally aged for 160 hr at 760°C (an upper operating temperature for the MSR), MC precipitated from the matrix according to the reaction

$$\text{M (soln)} + \text{C (soln)} \rightarrow \text{MC (ppt)} . \qquad (1)$$

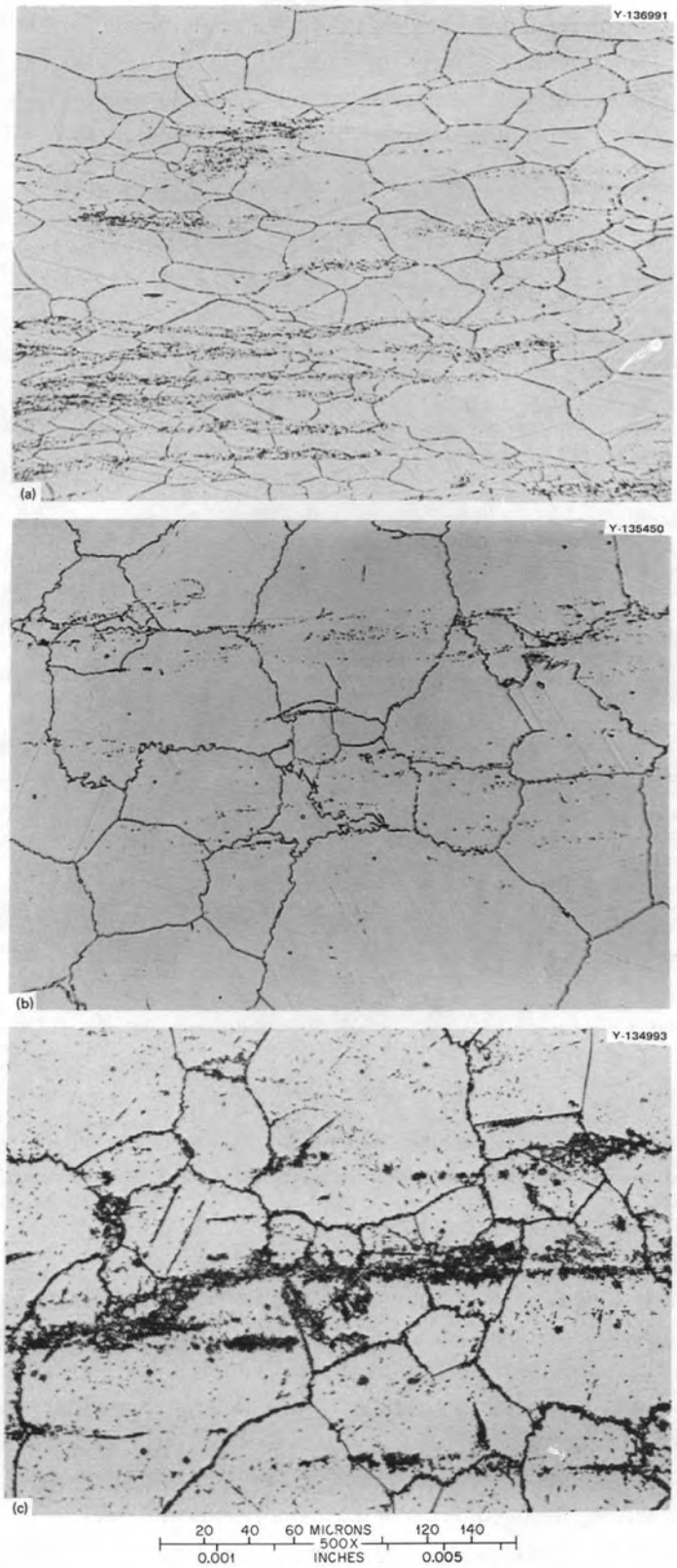

Fig. 1. Optical photomicrographs illustrating the "memory effect" in alloy 452. (*a*) As swaged, (*b*) after 1 hr at 1177°C, (*c*) after 1 hr at 1177°C + 160 hr at 760°C.

Figure 1(*c*) shows that the precipitation of carbide occurred predominately in the same areas where it existed after swaging, thus revealing a "memory effect."

A more detailed picture of this memory effect was obtained using TEM. Figure 2 shows a micrograph of a foil prepared from alloy 452 after the aging treatment at 760° C. The large "primary"

Fig. 2. Transmission electron micrograph showing MC-type precipitates in alloy 452 after annealing at 1177°C for 1 hr and aging at 760°C for 160 hr.

MC particle was one that failed to dissolve during the solution anneal. Other fine MC particles reprecipitated out in a stacking-fault morphology of (111) matrix planes. The mechanism of this type of precipitation was studied in detail by Silcock and Tunstall.[11] Even though the MC takes a different morphology upon aging, it does so in the same general location in the matrix. Precipitation of MC during aging did not always occur in a stacking-fault morphology. Sometimes the MC formed thin platelets on dislocations along the {111} matrix planes as shown in Fig. 3. The relation of the MC platelets to the matrix was epitaxial, that is, $(111)_{MC} \| (111)_{\gamma}$.

The main point regarding the elimination of the memory effect in Ti–Hastelloy N alloys is that resolution of the carbides is not enough; the solute elements must also be dispersed uniformly.

11. J. M. Silcock and N. J. Tunstall, "Partial Dislocations Associated with NbC Precipitation in Austenitic Stainless Steels," *Philos. Mag.* **10**, 360–89 (1964).

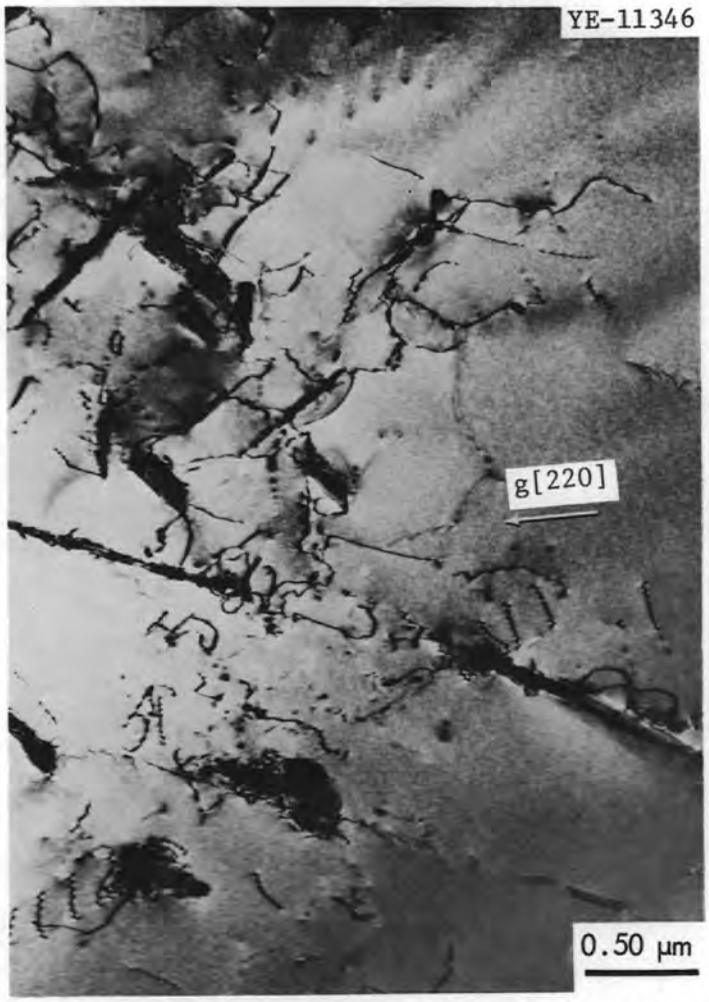

Fig. 3. Transmission electron micrograph showing MC platelets lying on {111} matrix planes in alloy 452. The sample had been annealed at 1177°C for 1 hr and aged at 760°C for 160 hr.

Adjustment of Carbon Content

The first step in adjusting the carbon content of the alloy was to estimate the solubility of carbon in Ti-modified Hastelloy N at 1177°C. The amount of carbon soluble in the alloy at 1125°C (~50°C below the standard annealing temperature) was estimated to be 0.045 wt % (see Appendix B). Thus, a 2% Ti–Hastelloy N alloy with less than 0.045 wt % C was expected to dissolve completely at 1177°C. Therefore, alloy 451 was prepared with a carbon content of 0.038 wt % and was fabricated into $^1/_4$-in.-diam rod according to the "standard" fabrication schedule for Hastelloy N given in Table 2. Even with this lower carbon content, the alloy contained a few carbide stringers after the standard fabrication procedure, as shown in Fig. 4(*a*). However, when the alloy with 0.038 wt % C was given a further 1-hr solution anneal at 1177°C, virtually all of the carbides were dissolved as shown in Fig. 4(*b*). Moreover, carbide stringers did not reappear after aging at 760°C for 223 hr, as shown in Fig. 4(*c*). Instead, carbide particles precipitated on grain boundaries, twin boundaries, and on {111} matrix planes. These metallographic results show that precipitates were present during fabrication of alloy 451, but were eliminated when small as-swaged samples of the same heat were solution annealed for 1 hr at 1177°C in the laboratory. We believe that the difference in results was due to the differences in quantity of material

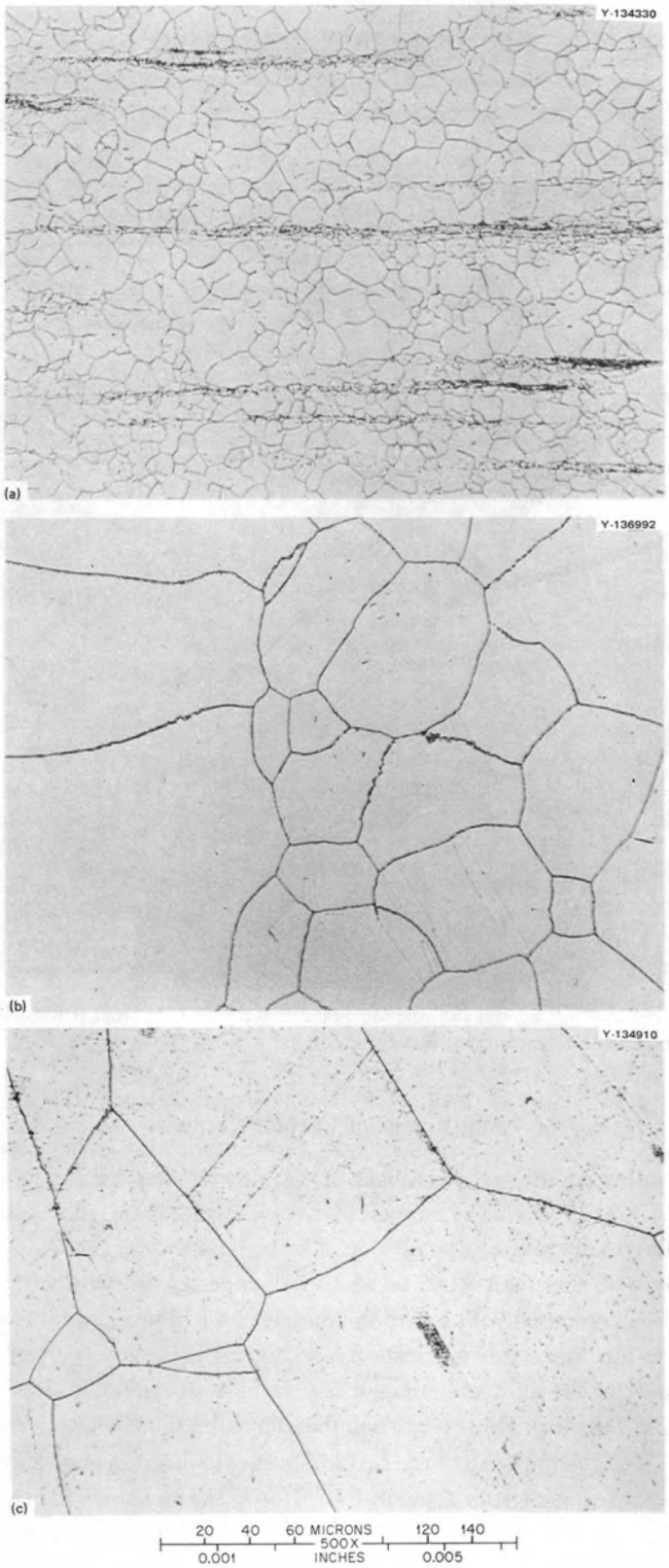

Fig. 4. Optical photomicrographs of alloy 451. (*a*) As-swaged condition, (*b*) after annealing 1 hr at 1177°C, (*c*) after annealing 1 hr at 1177°C followed by 223 hr at 760°C.

treated and in their respective cooling rates. The probability of carbide precipitation would be higher with larger quantities of materials, since the larger mass would cool more slowly in air. That is, larger samples see longer times in the temperature range ≈500 to 1000°C, where MC precipitation can take place.

The rate of carbide dissolution in alloy 451 was compared quantitatively with that in alloy 452, which has a higher carbon content. This was accomplished by annealing samples of each at 1177°C in argon for different times up to 8 hr and then cooling them in an argon stream. Electrochemical extraction techniques were then used to measure the quantity of undissolved carbide left in the microstructure. The results of this experiment are given in Fig. 5. As might be expected, complete

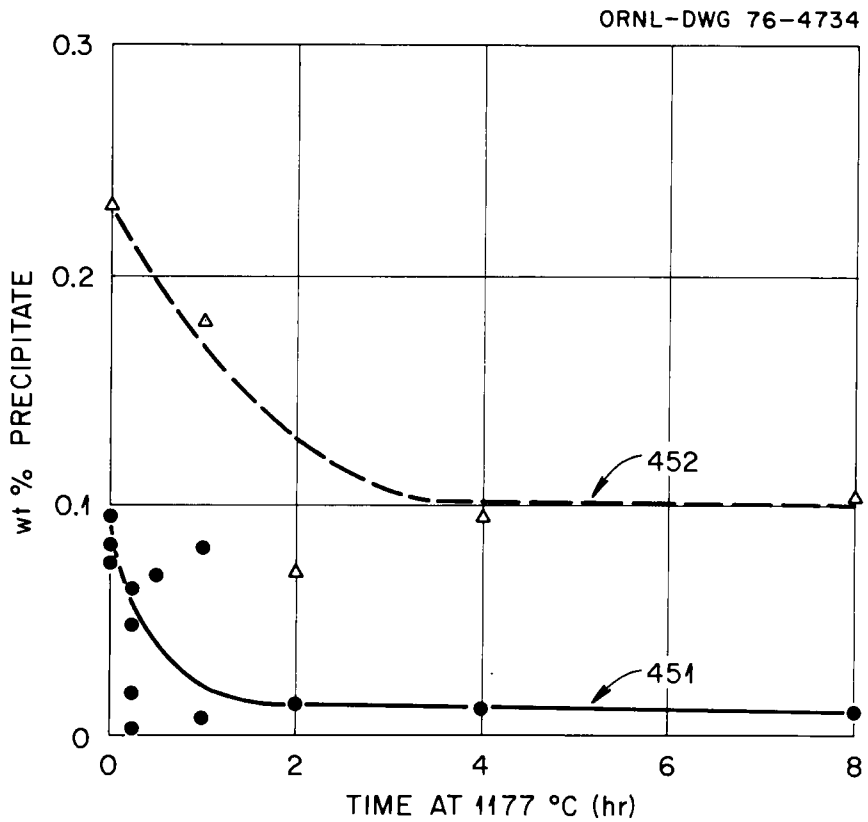

Fig. 5. Amount of MC precipitates remaining in alloys 451 and 452 as a function of solution annealing time at 1177°C.

solution is achieved much more rapidly in alloy 451, because of the lower carbon content, than in alloy 452. In the case of 451, about 1 hr was needed to dissolve the precipitate remaining in the alloy after the "standard" fabrication. In other words, for annealing times less than 1 hr, the reaction

$$\text{MC (ppt)} \rightarrow \text{M (soln)} + \text{C (soln)} \tag{2}$$

was incomplete. For times greater than ~1 hr, essentially all of the carbides were dissolved by the matrix. The small amounts of carbide, which were extracted following the longest annealing time, precipitated during cooling.[12] The results for 452 show that its higher carbon content produced greater amounts of carbides in the microstructure than did 451 for all annealing times investigated at 1177°C. This meant

12. D. J. Bradley and J. M. Leitnaker, private communication (1975).

that higher temperatures or longer times at 1177° C would be needed to eliminate completely the stringers from Ti–Hastelloy N with 0.060 wt % C. However, our calculations (Appendix B) show that with 0.06 wt % C and 2 wt % Ti, the MC will never dissolve completely at 1177° C.

Adjustment of Fabrication Parameters

Minor changes in annealing time, as in the case of fabricating 452 (see Table 2), were unsuccessful in removing carbide stringers from the microstructure [see Fig. 1(*a*)]. Samples of the as-swaged 452 were annealed for 1 hr at 1177, 1204, 1260, and 1300° C, respectively, and then aged at 760° C for 160 hr. The microstructures produced by these heat treatments are shown in Fig. 6. Solution annealing at 1177° C [Fig. 6(*a*)] and 1204° C [Fig. 6(*b*)] did not eliminate the memory effect, and many carbides reprecipitated in areas originally containing stringers. However, the anneals at 1260° C [Fig. 6(*c*)] and 1300° C [Fig. 6(*d*)] were successful in removing the stringers. The microstructure contained primarily a fine Widmanstätten structure of MC within the grains, but some MC particles were also observed in the grain boundaries. The habit planes for the precipitation were again the matrix {111} planes, and the relationship between MC and matrix was again epitaxial, that is, $(111)_{MC} \| (111)_{\gamma}$. Although much of the precipitate in the sample annealed at 1204° C [Fig. 6(*b*)] had the Widmanstätten morphology, many precipitates were still concentrated in original stringer areas. This observation strongly suggested that while most of the carbides were dissolved at 1204° C, a 1-hr annealing time at this temperature was not sufficient to permit adequate homogenization of the carbide-forming elements throughout the matrix.

From the results of annealing experiments on alloy 452, a new fabrication schedule was designed which produced a microstructure without stringers in an alloy containing ~0.060 wt % C. The pilot run of this new schedule is given in Table 2 for alloy 450. The material was consolidated and drop cast into a 6-in. × 1-in.-diam cylindrical ingot as described previously. The 450 ingot was then canned in type 316 stainless steel to minimize decarburization during processing at high temperatures in air. The microstructure of the as-cast ingot contained irregular-shaped grains with segregated patches of carbide particles, see Fig. 7(*a*). Hot swaging was conducted at 1177° C, as before, but the reheat times were held to 15 min to minimize grain growth. After hot swaging, the microstructure contained a fine-grain structure with carbides in the grain boundaries as shown in Fig. 7(*b*). Work with Ti–Hastelloy N at this laboratory, as well as work by others[13,14] with different nickel-base alloys, has shown that MC particles very effectively inhibit grain growth. Areas lacking in carbides experienced more grain growth, and hence a duplex grain structure was produced. The swaged rod was annealed at 1260° C for 1 hr, which dissolved most of the carbides and produced large recrystallized grains [Fig. 7(*c*)]. However, enough carbides remained to justify an additional anneal of 1 hr at 1300° C. The samples were quenched in water after the 1300° C anneal to prevent precipitation of carbides during cooling. This latter anneal was effective in dissolving essentially all of the carbides as shown in the micrograph in Fig. 7(*d*). We believe that the discrepancy between the results of a 1-hr anneal at 1260° C for small samples of both the 452 and the 450 ingots was again the result of insufficient annealing in the fabrication furnace. The discrepancy points out the need for careful quality control in fabricating Ti–Hastelloy N. The next three micrographs in Fig. 7 show the material after cold swaging [Fig. 7(*e*)], a subsequent 15 min at 1177° C stress relief anneal [Fig. 7(*f*)], and after final cold swaging [Fig. 7(*g*)]. During these final steps the grain size was reduced through cold-work and recrystallization processes. Finer grain sizes could have been obtained

13. M. J. Donachie, A. A. Pinkowish, W. P. Danesi, J. F. Radavich, and W. H. Couts, "Effect of Hot Work on the Properties of Waspaloy," *Metall. Trans.* 1, 2626–27 (September 1970).

14. W. Betteridge, *The Nimonic Alloys,* Edward Arnold, London, 1959, p. 102.

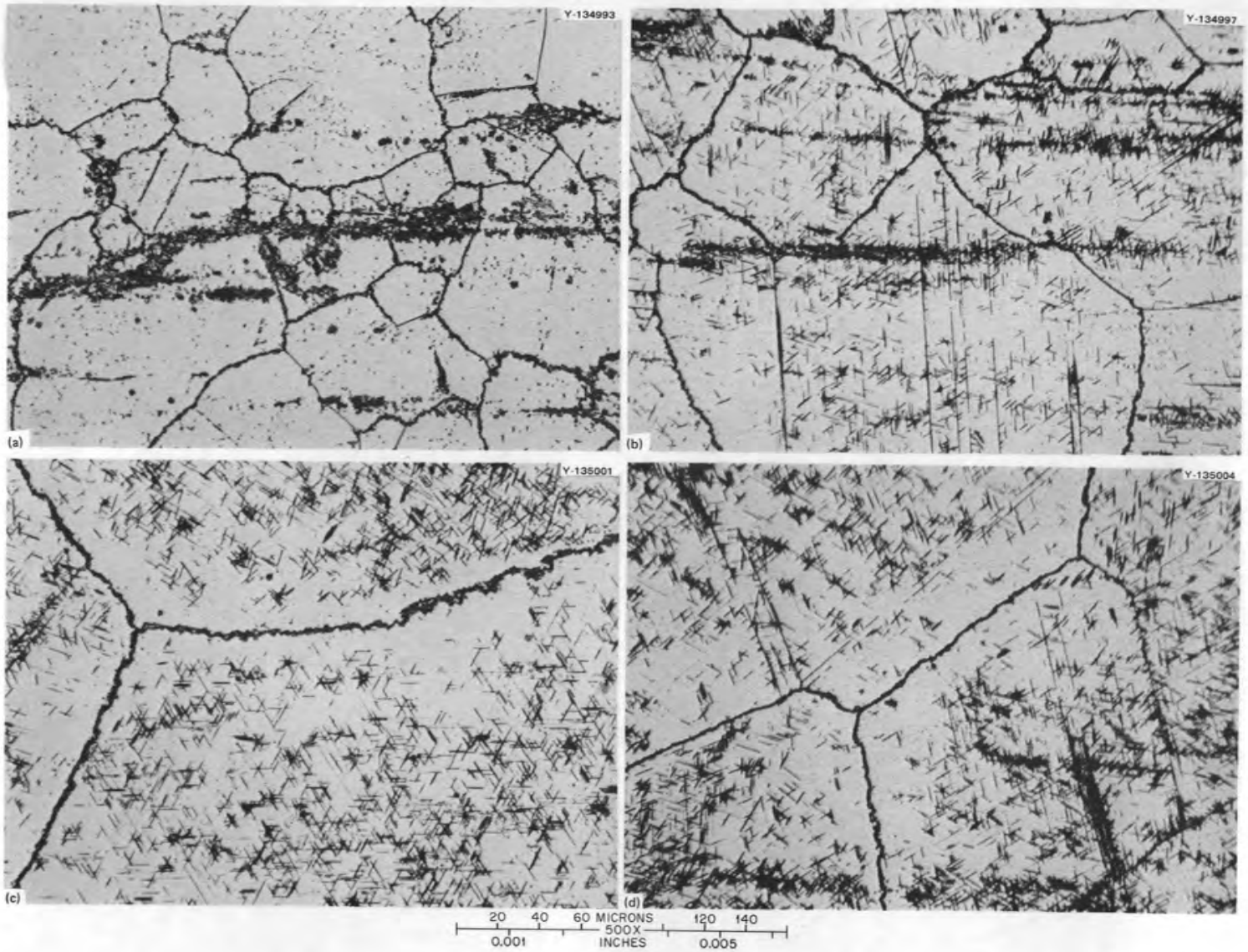

Fig. 6. Photomicrographs showing elimination of "memory effect" in alloy 452 (0.055 wt % C) by increasing the solution annealing temperature. (*a*) 1 hr at 1177°C + 160 hr at 760°C, (*b*) 1 hr at 1204°C + 160 hr at 760°C, (*c*) 1 hr at 1260°C + 160 hr at 760°C, (*d*) 1 hr at 1300°C + 160 hr at 760°C.

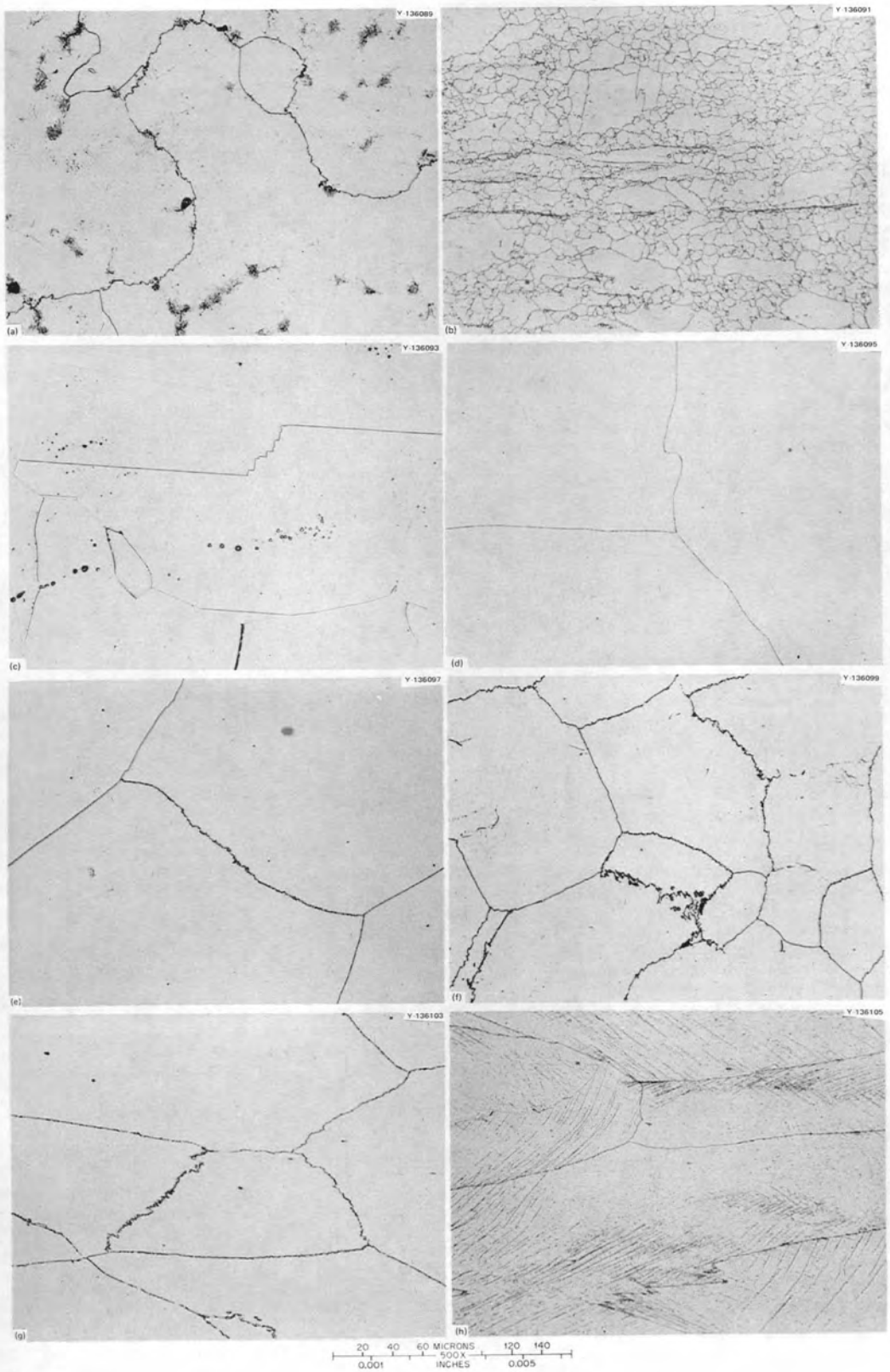

Fig. 7. Photomicrographs of alloy 450 at various stages of fabrication by a process designed to eliminate carbide stringers. (*a*) As cast, (*b*) after hot swaging at 1177°C, (*c*) solution annealed 1 hr at 1260°C, (*d*) annealed 1 hr at 1300°C and water quenched, (*e*) 39% reduction in area by cold swaging, (*f*) annealed 15 min at 1177°C, (*g*) 45% reduction in area by cold swaging (finished ¼-in.-diam rod), (*h*) aged 168 hr at 760°C.

by recrystallizing at lower temperatures. A few carbides were precipitated in the grain boundaries of the final product but no stringers were observed. As final proof that the memory effect had been eliminated, an as-swaged 450 sample was aged at 760° C for 168 hr. The microstructure after aging was found to contain a fine Widmanstätten structure of thin MC platelets lying along crystallographic directions as shown in Fig. 7(*h*). Transmission electron microscopy again showed that the platelets were stacking-fault precipitates lying on {111} matrix planes with $(111)_{MC} \| (111)_{\gamma}$. Note the absence of any stringers in the microstructure.

Precipitate extraction data from samples selected during the fabrication of both 452 and 450 are compared in Fig. 8. These data also show how the memory effect was removed from Ti–Hastelloy N. Alloy 450, which contained slightly more carbon than 452, initially contained slightly greater quantities of MC. Some precipitation of MC occurred during the hot swaging of both alloys. Solution annealing was a critical step in eliminating the memory effect, since substantially more carbides were dissolved in alloy 450 because of higher solution annealing temperatures. After solution annealing, the extracted amounts of carbides remained esentially unchanged through the remaining steps for both alloys. It is worth noting that a high-temperature anneal could remove stringers from either 452 or 450 after fabrication was completed, but the material would end up with a very large grain size. By performing the high-temperature anneal early in fabrication, it is possible to control grain size during the latter steps by carefully selecting the degree of cold-work and recrystallization temperatures.

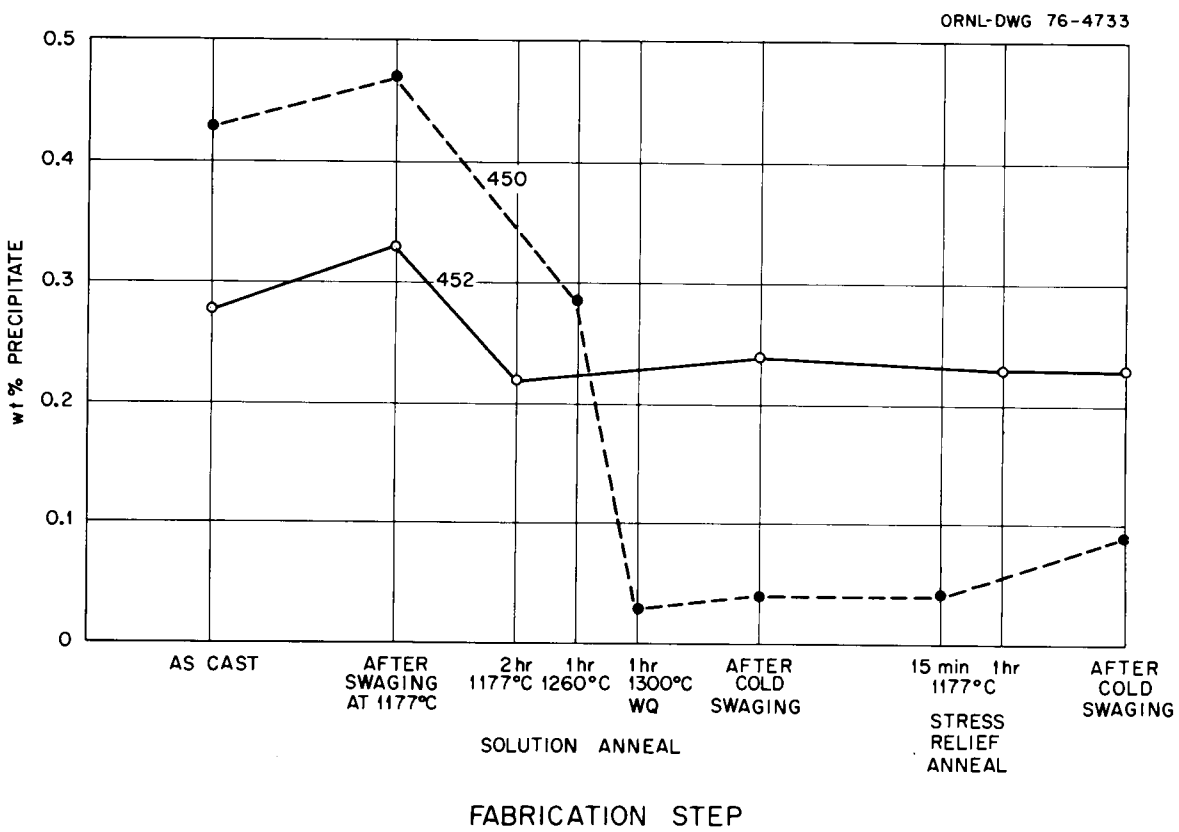

Fig. 8. Amount of MC precipitate remaining in microstructure of alloys 450 and 452 after various steps during fabrication.

PROPERTIES OF HOMOGENEOUS Ti-HASTELLOY

In order to determine whether Ti–Hastelloy N with a more homogeneous microstructure was an improvement over the previous heats of the alloy, it was subjected to neutron radiation and corrosion tests. Irradiation testing consisted in exposing 2-in. (5-cm) tensile specimens to a thermal neutron fluence of 3×10^{20} neutrons/cm^2 in the Oak Ridge Research Reactor at temperatures of 650, 704, and 760° C for about 1000 hr. The specimens were all subsequently creep tested at 650° C. Earlier results, also at 650° C, on Ti–Hastelloy N containing carbide stringers are given in Fig. 9,

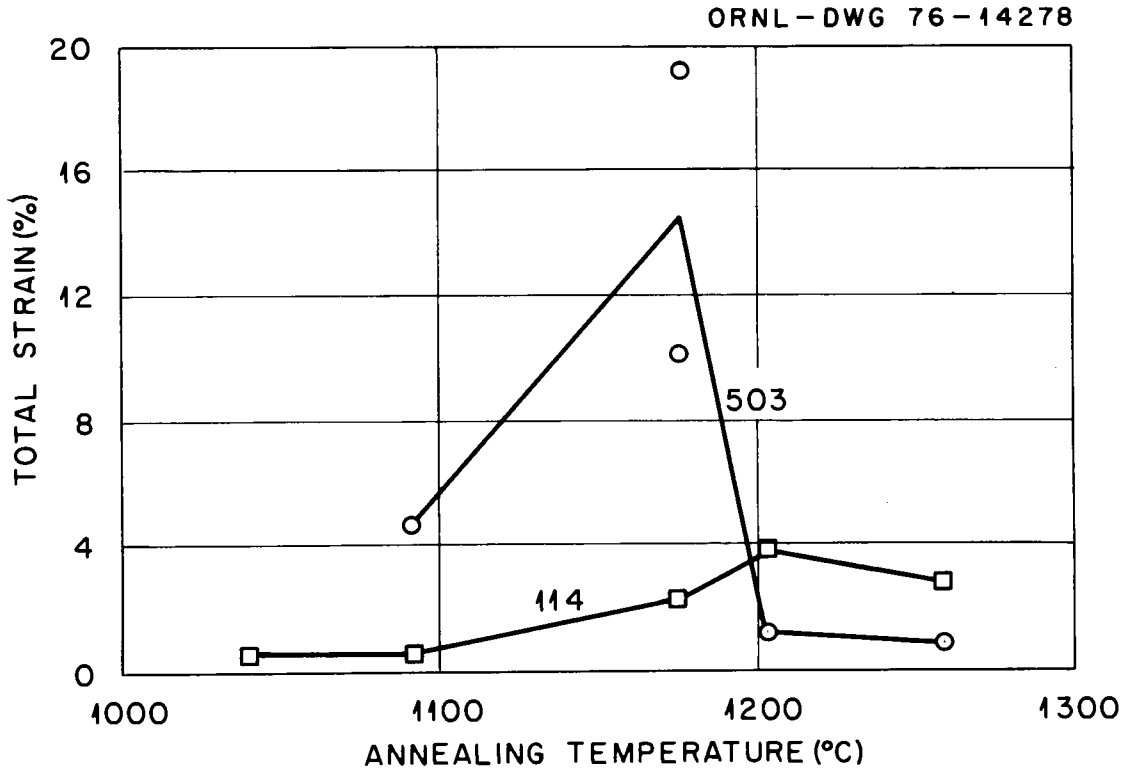

Fig. 9. Effect of annealing temperature on postirradiation creep ductility at 650°C of two Ti–Hastelloy N alloys having the same nominal composition.

with the total strain (ductility) of the specimen at rupture plotted as a function of the solution annealing temperature. The 1-hr solution anneals were given to the specimen just prior to exposure in the ORR. There are two points to be made concerning these data. First, there was a wide variation in postirradiation ductility between alloys with the same nominal composition (see Table 1); second, there was a large scatter of data between specimens of the same heat. This second point was particularly obvious in the data for alloy 503 at 1177 and 1204° C. There was both a spread in data for supposedly identical samples (data at 1177° C) and an unreasonable drop in ductility when going from a solution annealing temperature of 1177 to 1204° C. Although the data are encouraging because they demonstrate that Ti–Hastelloy N can be produced with good resistance to radiation damage (e.g., the 503 samples annealed at 1177° C), the large variation and scatter prevent one from learning how to do it. Furthermore, such variation in properties would probably be unacceptable for nuclear-grade components. When the microstructure is relatively homogeneous, as in the case of specially fabricated heat 450, the scatter in postirradiation creep ductility was significantly reduced. This result is demonstrated in Fig. 10, with total strain plotted as a function of annealing time at one

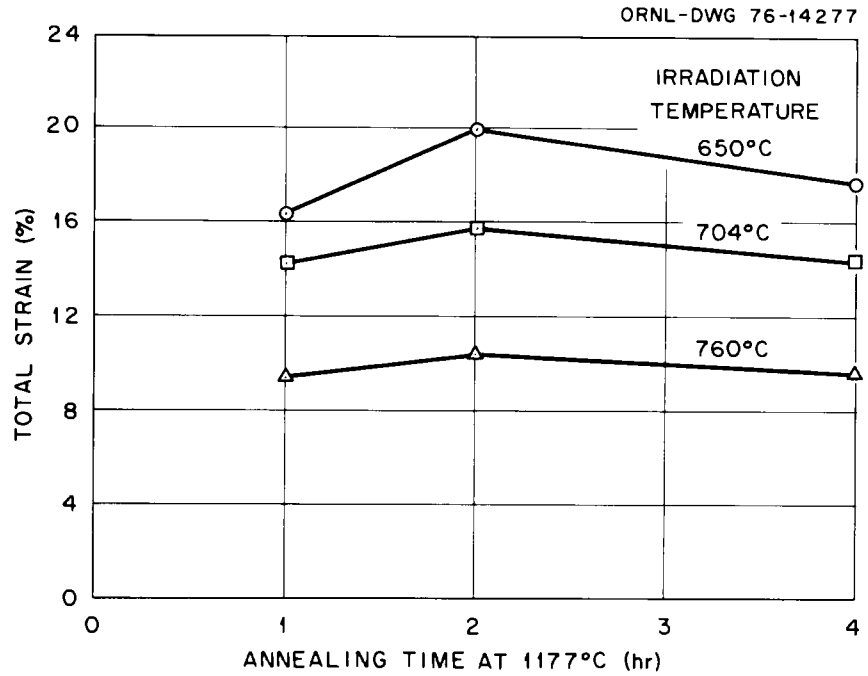

Fig. 10. Effect of annealing time at 1177°C on the postirradiation creep ductility of homogeneous Ti–Hastelloy N alloy 450.

"solution" annealing temperature of 1177°C. It is important to point out that the 450 specimens were homogeneous *before* the anneal and that the series really compares specimens with different grain sizes and not different degrees of carbide dissolution as in Fig. 9. The test series also shows the effect of irradiation temperatures on the resulting creep ductilities. The main point is that the homogeneous specimens were extremely well behaved, with little variation in the data. In fact, one is able to pick out an optimum annealing time of 2 hr, which is consistent for all three irradiation temperatures. Beyond 2 hr the ductilities were probably lower because of the increases in grain size. Stress rupture data for 450 (see Fig. 11) also showed relatively low scatter and demonstrated that the alloy was generally superior to other Ti–Hastelloy N alloys which contained stringers.

Preliminary results of tellurium corrosion tests for alloy 450 also indicated that a homogeneous microstructure was beneficial. Table 3 compares crack data collected from three Hastelloy N alloys that were exposed to tellurium vapor at 700°C and subsequently tensile tested at room temperature. Heat 450 specimens had less cracks per unit length, and the cracks were shallower than either the unmodified (heat 5065) or Ti–Hastelloy N (heat 114), both of which contained stringers. Although the yield and ultimate strengths for the 450 specimen were generally the same as for 5065 and 114, its ductility was greater.

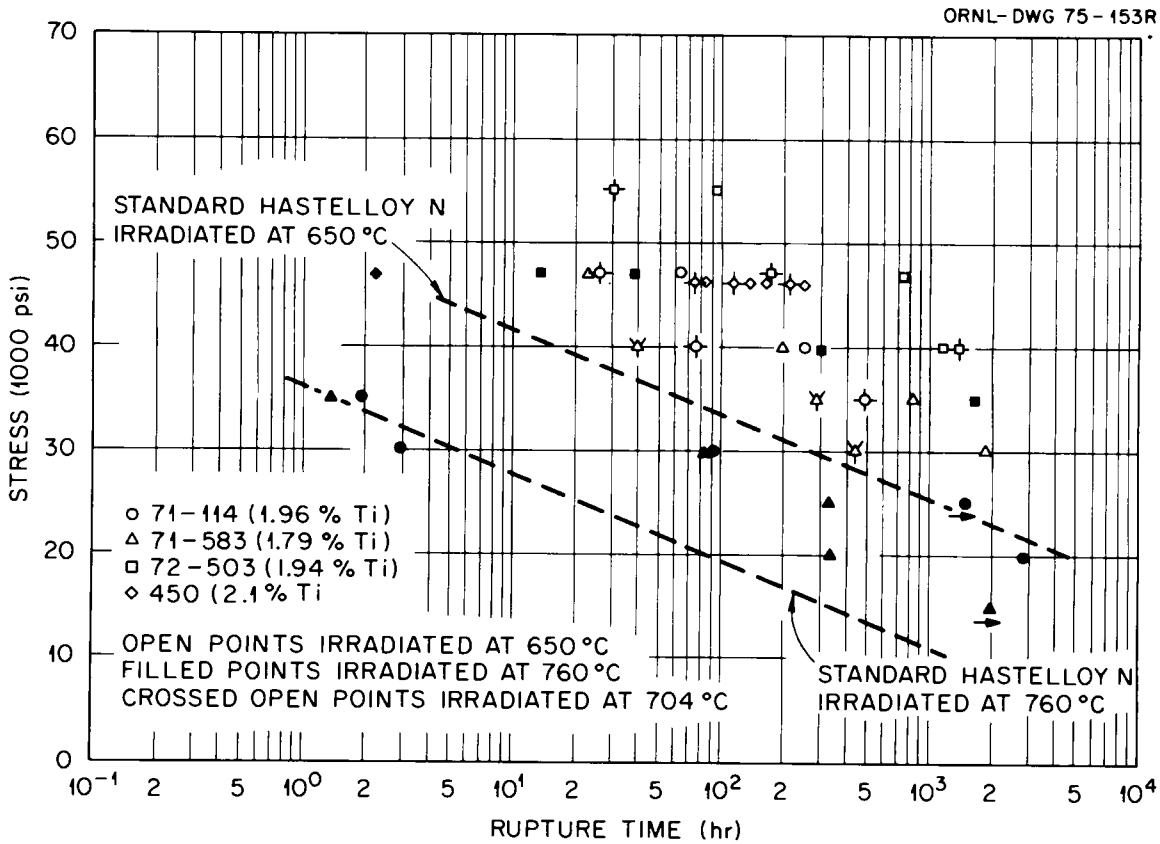

Fig. 11. Postirradiation creep properties of Ti–Hastelloy N alloys at 650°C. Thermal fluence of irradiation = 3×10^{20} neutrons/cm^2.

Table 3. Preliminary results of tellurium corrosion tests

(250 hr in Te vapor at 700°C, followed by tensile testing at room temperature)

Alloy heat No.	Cracks/in.	Average depth (μm)	Maximum depth (μm)	Yield strength (ksi)	Ultimate tensile strength (ksi)	Uniform elongation (%)
5065	240	44.5	89.9	52.5	125.7	38.5
114	225	56.8	120.0	48.6	111.2	49.9
450	127	21.9	58.4	50.1	112.1	55.7

DISCUSSION

The present work describes the conditions necessary to produce a homogeneous, "stabilized" nickel-base alloy on a practical scale; the best procedure is to eliminate, as much as possible, the presence of second phases during the hot reduction steps. However, if this is not done successfully, homogeneity can be subsequently achieved by annealing at high temperatures—but only with some difficulty.

It is clearly not enough to "solution treat" a nickel-base alloy at 1177°C for 1 hr and obtain a homogeneous material. Disappearance of the stringers is not sufficient to gain homogeneity; the stringer constituents must be sufficiently dispersed to erase the memory effect.

Furthermore, there is no reason to expect that 1 hr at any particular temperature below the melting point would suffice to homogenize a particular sample. Rather, the amount of time required will depend strongly on the kinds and amount of elements present as well as on the previous history of the sample.

These statements are applicable not only to "stabilized" alloys but to alloys in general. The alloys which tend to form MC-type precipitates are particularly easy to handle conceptually (see Appendix B), but the same principles apply to all alloys fabricated from massive, cast structures.

From the fabricator's standpoint, lowering the amount of the "stabilizing" element, or carbon, or both will make the fabrication easier, while still obtaining a homogeneous alloy. The annealing temperature can be lower than with the higher concentrations, without precipitating any carbides. From the user's standpoint, the smaller amount of carbide precipitate, overall, is actually a help rather than a hindrance. The formation of deleterious stringers is avoided, and the strengthening advantage of a homogeneous distribution of carbide precipitates is still achieved. On the other hand, raising the temperature during hot fabrication procedures will permit the presence of increased concentrations of carbide-forming elements in the matrix, thus providing a greater source of precipitates for increasing the strength of the material.

The "memory effect" is worth special mention. Even though the elements of the alloy are taken into solution before fabrication, precipitation can still take place in unwanted "stringer" morphology during hot working or during cooling via the "memory effect." The elements important in forming MC-type carbides will not all diffuse at the same rate. Those diffusing most slowly can remain in the general area of their previous location, even though in solution, and cause reprecipitation in the same area. Only direct experimentation can reveal whether homogenization has been complete enough to remove vestiges of this effect. It is, therefore, better to eliminate the presence of second phases as completely as possible during fabrication.

The creep tests on irradiated specimens clearly show that Ti–Hastelloy N samples with a homogeneous microstructure perform in a much more consistent manner, with less scatter in results. Therefore, it is reasonable to believe that the use of homogeneous alloys would be advantageous from the standpoint of both alloy development and the final application. That a homogeneous microstructure appears to also improve the alloy with regard to both resistance to radiation and tellurium attack is an added bonus.

CONCLUSIONS

1. Carbide stringers form during the fabrication of Ti–Hastelloy N alloys, as in many other structural materials, because of failure to remove the original segregated carbides (from casting) before processing and/or the precipitation of carbides during hot working.

2. The carbides in Ti–Hastelloy N are identified as fcc MC type with a composition close to $MC_{0.65}$, where M is mainly Mo, Ti, and Cr in decreasing order.

3. A "memory" effect has been observed in the solution-annealed and aged Ti–Hastelloy N alloys such that carbides reprecipitate in a stacking-fault morphology in the same areas which originally contained stringers. This effect reflects a nonhomogeneous, that is, only a very local, distribution of metallic elements caused by insufficient solution annealing treatment.

4. A homogeneous Ti–Hastelloy N can be produced by lowering the carbon content of the alloy from ~0.060 to ~0.038 wt % while using the usual fabrication schedule. In this case, the standard 1 hr at 1177°C solution annealing treatment is capable of distributing the carbide-forming elements uniformly.

5. A homogeneous alloy can also be produced in Ti–Hastelloy N alloys with higher carbon contents (~0.060 wt %) by increasing the solution annealing temperature to ~1300°C. The high-temperature solution anneal should be given early in fabrication so that a small, final grain size can be achieved during subsequent cold swaging and annealing.

6. For a solution annealing treatment to be effective in producing a homogeneous alloy it must:

a. Dissolve the carbides.
b. Be of sufficient duration to alloy the carbide-forming elements to disperse, by diffusion, uniformly throughout the alloy.
c. Take into account the dimensions of material being treated, reflecting the cooling behavior and the time that a substantial fraction of the alloy is in a carbide-precipitation temperature range.

7. In aged Ti–Hastelloy N alloys where the memory effect was eliminated, the MC-type carbides formed a fine uniform Widmanstätten structure of MC (stacking-fault precipitates) lying epitaxially on the {111} planes of the matrix such that $(111)_{MC} \| (111)_{\gamma}$. Some small carbide particles were also observed in the grain boundaries.

8. The variation in postirradiation properties of Ti–Hastelloy N was significantly reduced by manufacturing a homogeneous alloy. A homogeneous microstructure also appeared to enhance the resistance of the alloy to both radiation damage and grain boundary embrittlement caused by tellurium.

ACKNOWLEDGMENTS

The authors gratefully acknowledge R. Heestand and his staff for fabricating the alloys, J. Feltner and B. McNabb for heat treating, K. Russell for metallography, and G. A. Potter for sample preparation and extractions. Many thanks also to K. Farrell and P. Sklad for reviewing the manuscript. The report was edited and prepared for reproduction by the Technical Publications Department.

APPENDIX A

The composition of the extracted carbide does not appear to be $MC_{1.0}$ (although insufficient precipitate has been extracted for a definitive value). This conclusion can be drawn from two lines of evidence: the x-ray lattice parameter and the amount of precipitate extracted from samples aged at temperatures between 650 and 760°C.

Samples of the alloys described here and heated at 1177°C yield precipitates with a lattice constant of 4.298 ± 0.005 Å. Storms[1] gives the lattice constant of $TiC_{1.0}$ as 4.328 Å, a value which decreases to approximately 4.26 Å at $TiC_{0.3}$.

1. E. K. Storms, *A Critical Review of Refractories,* LA-2992 (August 1964).

The precipitate is more complicated than the titanium-carbon compound TiC_x. It contains approximately 60 wt % Mo, 10 wt % Cr, and only 30 wt % Ti (0.43, 0.13, and 0.43 atom fraction respectively). Thus, one cannot use the data given by Storms directly to estimate a carbon-to-metal ratio.

One might suppose that the presence of molybdenum in the MC_x lattice would expand the dimension over that of TiC. That is, Slater[2] indicates the radius of titanium is 1.40 Å, while that of molybdenum is given as 1.45 Å. However, the molybdenum carbide which is face-centered cubic, β-Mo_3C_2, has a lattice parameter of 4.28 Å.[1]

To estimate the lattic constant of an (Mo,Ti)C phase, one might use a linear extrapolation between $TiC_{1.0}$ and $MoC_{0.67}$, by combining the chromium with the molybdenum in this case. Such an extrapolation yields a lattice constant of 4.301 Å [which is 4.281 + 0.43(4.328 − 4.2810) Å]. This is only slightly greater than the lattice constant found. The carbon content based on a similar interpolation between $TiC_{1.0}$ and $MoC_{0.67}$ would correspond to $MC_{0.81}$.

The formula of the precipitate can also be established via another route. Long-time aging (1000 hr) at 650°C of cold-worked samples yielded a 0.62 wt % precipitate. The lattice parameter of the precipitate was the same as that for the precipitate from samples heated at 1177°C, although an asymmetry of the x-ray lines (to higher 2θ values) was observed. Assuming *all* of the carbon in the sample, 0.06 wt %, is in the precipitate, 0.56 wt % of the sample is in the metallic portion of the precipitate. Thus, one has approximately 8.1×10^{-3} g-atom of metal combined with 5.0×10^{-3} g-atom of carbon, corresponding to a formula of $MC_{0.62}$.

The results of both calculations indicate a carbon-to-metal ratio considerably less than unity; the lower value is probably more reliable since it is based on analysis. There is some uncertainty in the carbon analysis on which the lower value is based. Thus we ascribe a value of 0.65 ± 0.10 to the carbon-to-metal ratio of the MC-type compound.

APPENDIX B

The purpose of the present study was not a precise determination of thermodynamic properties in the titanium-modified Hastelloy N system; nevertheless, the auxiliary data obtained to facilitate the study may be usefully expressed in a thermodynamic form. These data served as the basis for designing the alloys reported in Table 1.

To avoid segregation in a "stabilized" alloy (as with titanium or niobium), precipitation of the carbide must be avoided. For the case of a titanium-modified alloy the requirement is often stated in thermodynamic terms as follows: For the reaction

$$\text{Ti (dissolved in alloy)} + \text{C (dissolved in alloy)} = \text{TiC (precipitate)}\ , \tag{B1}$$

the equilibrium constant, K, is given by

$$K = a_{TiC}/a_{Ti}a_C\ , \tag{B2}$$

where a is the thermodynamic activity of the species indicated and cannot be exceeded at any given temperature.

2. J. C. Slater, "Atomic Radii in Crystals," *J. Chem. Phys.* **41**, 3199–3204 (1964).

For reaction (B1), Eq. (B2) is rigorously correct, but in practice a simpler approach can be used. That is, a "solubility product" can be used if one does not vary the concentrations of the constituents too greatly. The appropriate statement is: the product

$$[\text{wt \% Ti}]\,[\text{wt \% C}]\ (=K') \tag{B3}$$

should not be exceeded in the alloy to avoid precipitation of the carbide.

The easiest way to establish the product K' at any temperature is to age a sample with a greater concentration of titanium and carbon than can be dissolved and determine the amount of each that has precipitated. The amount left in the alloy defines the product that must not be exceeded.

To determine K' [Eq. (B3)], alloy 503 (Table 1) was aged at 1177°C and extracted as described in "Materials and Experimental Procedures." The aging procedure was done so as to approach equilibrium from two directions. That is, samples were heated at a low temperature (1000°C) to precipitate more material than in the equilibrium state at 1177°C, and were also heated at a high temperature (1260°C) to dissolve more than the equilibrium amount at 1177°C. Then both samples were heated at 1177°C for 2 hr. The results are described in Table B1, which shows that between 0.12 and 0.20 wt % precipitate exists at 1177°C, or 0.16 ± 0.04 wt %. Thus the amount of titanium in solution in the alloy is $1.94 - (0.3 \times 0.16)$ or 1.89 wt %, where 1.94 is the amount of titanium, total, in the alloy (Table 1); 0.3 is the fraction of the metallic constituent in the precipitate that is titanium (Appendix A); and 0.16 is the wt % of precipitate. In Appendix A it was assumed that 0.06 wt % C was contained in 0.62 wt % precipitate extracted after 1000 hr at 650°C. Therefore the amount of carbon in the precipitate is $0.06/0.62 \times 0.16$, or 0.015 wt %, and the amount left in solution is $0.06 - 0.015$, or 0.045 wt %. The solubility product, K', as defined in Eq. (B3) is

$$[0.045]\,[0.189] = 0.0850\ ;$$

at 1177°C this product must not—or really, cannot—be exceeded. If the product for the total alloy is greater than this, precipitation will occur.

Table B1. Precipitation in alloy 503 after various heat treatments

Heat treatment	Precipitate (wt %)
16 hr at 1000°C	0.42
16 hr at 1000°C + 2 hr at 1177°C	0.20
16 hr at 1000°C + 1 hr at 1260°C	0.04
16 hr at 1000°C + 1 hr at 1260°C + 2 hr at 1177°C	0.12
1 hr at 1177°C	0.14

INTERNAL DISTRIBUTION

1–2. Central Research Library
3. Document Reference Section
4–8. Laboratory Records Department
9. Laboratory Records, ORNL RC
10. ORNL Patent Office
11. J. Bentley
12. E. E. Bloom
13. D. J. Bradley
14–23. D. N. Braski
24. R. W. Carpenter
25. J. V. Cathcart
26. R. E. Clausing
27. F. L. Culler
28. J. E. Cunningham
29. R. G. Donnelly
30. K. Farrell
31. G. M. Goodwin
32. R. J. Gray
33. M. L. Grossbeck
34. W. O. Harms
35. R. L. Heestand
36–38. M. R. Hill
39. J. A. Horak
40. H. Inouye
41. E. A. Kenik
42. Walter Kohn
43–47. J. M. Leitnaker
48. L. K. Mansur
49. P. J. Maziasz
50. H. E. McCoy
51. C. J. McHargue
52. R. E. McDonald
53. L. E. McNeese
54. John Moteff
55. N. H. Packan
56. P. Patriarca
57. H. Postma
58. T. C. Reiley
59. A. F. Rowcliffe
60. G. M. Slaughter
61. P. S. Sklad
62. J. O. Stiegler
63. D. B. Trauger
64. J. R. Weir
65. C. L. White
66. F. W. Wiffen
67. R. O. Williams

EXTERNAL DISTRIBUTION

68. Leo Brewer, Inorganic Materials Division, Lawrence Berkeley Laboratory, Berkeley, CA 94720
69. C. R. Brooks, Department of Chemical and Metallurgical Engineering, University of Tennessee, Knoxville, TN 37916
70. B. T. Frost, Director, Materials Science Division, Argonne National Laboratory, 9700 South Cass Avenue, Argonne, IL 60439
71. W. D. Manly, Stellite Division, Cabot Corporation, 1020 Park Avenue, Kokomo, IN 46901
72. T. E. Mitchell, Dept. of Met. and Mat. Sci., Case-Western University, Cleveland, OH 44106
73. B. F. Oliver, Department of Chemical and Metallurgical Engineering, University of Tennessee, Knoxville, TN 37916
74. J. W. Prados, Vice-President of Academic Affairs, University of Tennessee, Knoxville, TN 37916
75. W. Schilling, Institut für Festkorperforschung, der Kernforschungsanlage, Jülich, D-517 1, Postfach 365, Germany
76. S. Spooner, Department of Chemical Engineering, Georgia Institute of Technology, Atlanta, GA 30332
77. J. E. Spruiell, Department of Chemical and Metallurgical Engineering, University of Tennessee, Knoxville, TN 37916
78. E. E. Stansbury, Department of Chemical and Metallurgical Engineering, University of Tennessee, Knoxville, TN 37916

79. H. Ullmaier, Institut für Festkorperförschung, Kernforschungsanlage, Jülich, D517, Jülich 1, Postfach 365, Germany
80. A. M. Weinberg, Institute for Energy Analyses, ORAU, Oak Ridge, TN 37830
81. USERDA, Division of Buildings and Industry, Conservation Administration, Washington, DC 20545

    R. Anderson

82. USERDA, Division of Conservation Research and Technology, Washington, DC 20545

    J. Neal

83–84. USERDA, Division of Fossil Energy Research, Washington, DC 20545

    A. Mills
    H. Frankel

85–89. USERDA, Division of Magnetic Fusion Energy, Washington, DC 20545

    K. M. Zwilsky
    T. C. Reuther
    O. Manly
    C. D. Henning
    C. Finfgeld

90–95. USERDA, Division of Physical Research, Washington, DC 20545

    J. S. Kane
    L. C. Ianniello
    D. Readey
    D. K. Stevens
    M. C. Wittels
    S. Wolf

96–98. USERDA, Division of Solar Energy, Washington, DC 20545

    H. R. Blieden
    M. P. Prince
    G. M. Kaplan

99–100. USERDA, Oak Ridge Operations Office, P.O. Box E, Oak Ridge, TN 37830

    Director
    Research and Technical Support Division

101–127. USERDA, Technical Information Center, Office of Information Services, P.O. Box 62, Oak Ridge, TN 37830

☆ U.S. GOVERNMENT PRINTING OFFICE: 1977-748-189/154